Paste 2012 — R.J. Jewell, A.B. Fourie and A. Paterson (eds)

doi:10.36487/ACG_rep/1263_16_Adkins

BASF novel flocculant technology in dynamic thickening operation

S. Adkins *BASF Construction Polymers GmbH, Germany*

A. Berger *BASF Construction Polymers GmbH, Germany*

J. Muhor *BASF SE, Germany*

G. Brodt *BASF SE, Germany*

I. Flanagan *BASF Performance Products plc, United Kingdom*

Abstract

Although thickener operations constantly strive to maximise their separation efficiencies through both engineering and reagent improvements, to date the rheological properties of the consolidated underflow within the thickener continues to constrain overall performance.

BASF is developing a novel flocculant technology (NFT). Through laboratory scale batch evaluations this technology has already been shown to offer effective flocculation performance, whilst increasing the rate of underflow consolidation and significantly reducing associated underflow yield stress.

This paper will present application data to confirm the suitability and to demonstrate the performance benefits that BASF NFT provides for dynamic thickener operations.

1 Introduction

It is well documented that polymeric flocculants improve the initial compaction of a consolidating thickener slurry through the formation of a continuous network structure based upon micron-sized aggregates (flocs). These are derived from interactions between the polymer and solid particles with the resulting flocculated particles settle faster than single solid particles because of their size. This results in the formation of a structured, compacted zone with an average volume fraction lower than that possibly achieved by a non-flocculated suspension. However, the consolidated bed also supports the formation of pathways between the flocs which facilitate further dewatering (Boger, 2009; De Kretser et al., 2003).

A previous publication demonstrated a ‘proof of concept’ relating to process improvements for gravity thickener operations. It was shown that the BASF NFT could maintain existing flocculant process benefits (including effective aggregate formation, overflow clarity and consolidation of solids), whilst significantly reducing the influence that conventional flocculants (based upon high molecular weight water soluble polymers) have on the rheological properties of the consolidated thickener underflow (Berger et al., 2011).

This paper will extend the original laboratory scale batch test work findings by comparing and contrasting the performances of conventional flocculant and BASF NFT treatments under dynamic pilot scale semi-batch and continuous operation treatment systems.

2 Experimental section

2.1 Pilot scale thickener

The dynamic thickener test work was performed using a 50 L pilot thickener supplied by AKW Equipment and Process Design (AKW). The thickener had four ‘horizontal’ rake arms; each arm containing two blades. Two rake arms were fitted with pickets to aid dewatering, as well as a central rake shaft with a 5 cm diameter. The central rake shaft was connected to a drive motor placed at the top of the thickener, which produced rake speeds between 1–3 rpm. A description of the equipment is given below in Figure 1.

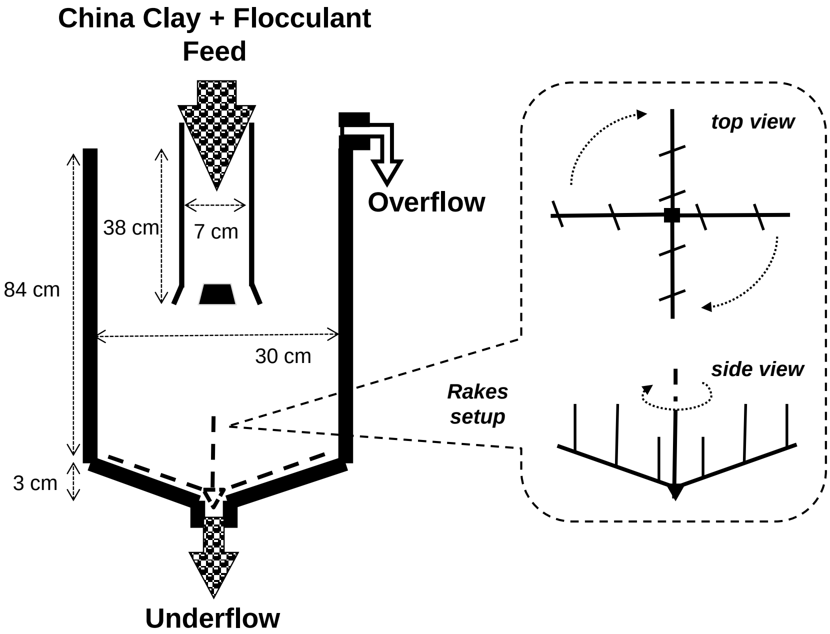

Figure 1 AKW Equipment and Process Design GmbH, AKA-SET pilot scale thickener schematic

2.2 Thickener operation

2.2.1 Flocculant feed

The flocculants were applied as solutions into the thickener feedwell using a standard peristaltic pump (Heidolph PD5201). Typical flow rates were in a range of 40–80 mL per minute.

2.2.2 Slurry feed

The slurry feed rate was controlled using a progressive cavity pump (Seepex Range BN), coupled with a flowmeter (Promag), typically operating between 200–250 L per hour.

2.2.3 Underflow pumping and sampling

The resultant underflow was pumped out of the thickener, using a peristaltic pump (Verder Dura 10) to minimise shear thinning and to mirror in situ underflow physical characteristics within a commercial thickener operation. The flow rates ranged between 8–12 L per hour and varied in proportion to the applied rake speed.

The underflow samples produced were subjected to minimal shear (in line with underflow raking) prior to rheological evaluations.

2.3 Pilot scale batch thickening process

Batch experiments applying conventional flocculant and BASF NFT were conducted for two reasons:

- To support previously reported laboratory scale batch data (Berger et al., 2011).
- To demonstrate a consistent and unambiguous differentiation between the solid-liquid separation performance within the thickening process and the rheology of the flocculated slurry produced by these two distinct flocculant technologies.

Batch thickening implies running the pilot thickener without underflow release, until the developing consolidated bed achieves a given depth (or height). The experiment involves continuous feeding of slurry and flocculant solution into the thickener feedwell, which had previously been filled with water. The underflow discharge point remained closed throughout the time that flocculated feed was introduced into the system. Flocculant/slurry conditioning took place within the feedwell forming aggregates (flocs) that freely settled to the bottom of the thickener. The rakes, which were maintained at a constant rotation speed, assisted the consolidation and dewatering of the aggregates, whilst the bed developed. The free water discharged to the overflow. This process was operated until a bed depth of 30 cm was achieved.

At this time the slurry and flocculant feed flows were stopped and the bed was raked for an additional 10 minutes to further improve dewatering and so enhance consolidation. Following this, the discharge valve was opened and outflow was controlled by a peristaltic pump (to minimise slurry shear thinning) and sub-sampled until a significant proportion of the available material was collected. The underflow pumping rate was set to be equivalent to the minimum volume of mud moved by the blades/rakes towards the discharge point for the given rake speed. Matching these criteria was crucial in order to produce samples and rheological data that were consistent and representative of the mud profile throughout the bed. All samples were immediately submitted for slump test, slurry specific density and subsequently for dry solids content determination.

The solids content (% w/w) versus slump diameter (mm) data for both conventional flocculant and BASF NFT treatments were plotted and compared against each other, as well as against the profile of the untreated China clay.

2.4 Pilot scale dynamic thickening process

The testing protocol was the same as that of the batch thickening, outlined in Section 2.3. However, once the required bed depth had been produced and the underflow pump started, treated feed slurry continued to be introduced into the system.

Underflow slurry samples were taken and characterised in the same manner as those within the previously reported pilot thickener batch operation.

2.5 Analytical measurements

2.5.1 Density

The density (g/cm^3) of the China clay slurry was determined using a densimeter (Anton Par DMA 35n). This is an effective tool to gain indirect ‘real time’ estimation of slurry solids content, thus informing the operator of underflow changes during the thickening process.

2.5.2 Solids content

The true solids contents (% w/w) were determined by oven drying the samples at 80°C for 12 hours.

2.5.3 Rheology

In this work the rheology of the material was assessed by performing a standard slump test with a small mould of circular cylindrical geometry (height = 50 mm, diameter = 50 mm), where the ‘spread’ (slump diameter - 2R - the final diameter of the collapsed sample) was taken as an indirect indication of the yield stress of the material (Figure 2). Note that a decrease in the slump diameter (spread) denotes an increase in yield stress and vice-versa.

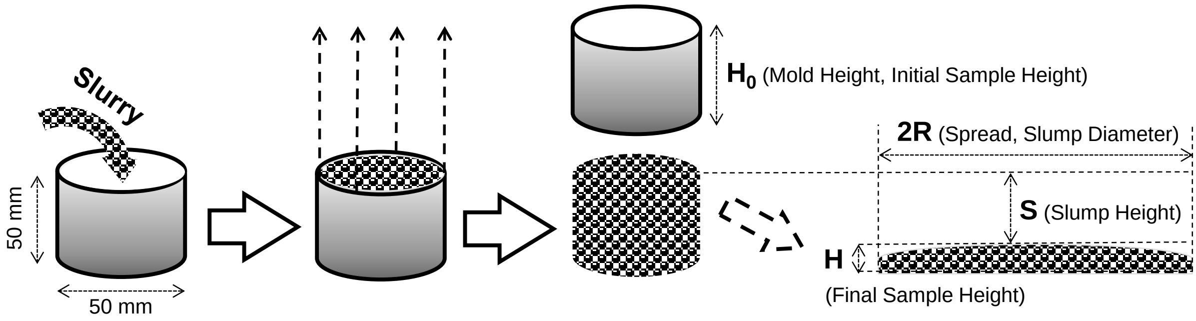

Figure 2 Schematic of the slump test

2.5.3.1 Slump test methodology

The slump test is a simple, time efficient, low cost and robust method of assessing the yield stress of suspended solids. It has been widely adopted in the cement industry to determine the 'workability' of fresh concrete and in the mining industry for monitoring and determining the rheology of slurries (Boger, 2009).

Several models relating the slump characteristic and the yield stress of materials have been developed using either a conical or cylindrical mould and a slump (slump height), spread (slump diameter) or both are measured and considered for predicting the yield stress. In most cases good agreement is obtained, however, some discrepancies between experimental and predicted slump characteristics still appear (Pashias et al., 1996; Clayton et al., 2003; Roussel and Coussot, 2005).

Pashias et al. (1996) have simplified the slump methodology by transposing the conical to a cylindrical geometry for the slump vessel and by establishing a simple equation for relating the slump height to the yield stress:

$$\boxed{\tau_{y'} = \tfrac{1}{2} + \tfrac{1}{2}\,.\sqrt{\mathbf{S'}}}$$

$$\tau_{y'} = \tau_y / \rho g \mathbf{H_0},\ \mathbf{S'} = \mathbf{S} / \mathbf{H_0} \qquad (1)$$

where:

$\tau_{y'}$ = dimensionless yield stress.

τ_y = yield stress.

ρ = material density.

g = gravity.

S′ = dimensionless slump height.

S = slump height.

H_0 = height of the mould or initial sample height.

Roussel and Coussot (2005) have extended this theoretical analysis by including different asymptotic flow regimes according to the ratio between the final radius (R = half of the slump diameter) and the final height (H) of the slumped sample, as follow:

- pure shear flow: H<<<R.
- pure elongational flow: R<<<H.

Particularly within our work, where the equipment, type and particle size of the material, as well as the conditions employed in the process, produced thickened, flocculated, China clay with low solids (<30% w/w) associated with low yield stresses (<10 Pa), a nearly pure shear flow regime seems to operate.

In other words, at this regime the depth of the sample layer is much smaller than its length characteristic (final sample height <<< slump diameter) and, as a result, the slump diameter (spread) appears to be the more relevant parameter for estimating the yield stress (Roussel and Coussot, 2005):

$$\tau_y = 225\rho g\Omega^2/128\pi^2\mathbf{R}^5 \quad (2)$$

where:

Ω = sample volume.

R = radius, half of slump diameter.

2.6 Applied slurry characteristics

The China clay slurry used was streamed from Amberger Kaolinwerke (Amberger) production line at their mine site in Hirschau, Germany.

The average particle size distribution was measured using a particle size analyser (Malvern Mastersizer 2000). The China clay used had particle sizes ranging between 11–13 µm (D: 0.63).

The pH of the slurry was 7 and the solids content was within the range of 1.0–1.2% w/w.

2.6.1 Rheological property of AKW's China clay

A sample of the untreated China clay feed was concentrated up to 50% w/w by vacuum filtration. The rheology of the concentrated China clay sample was then assessed by proceeding with direct yield stress (Pa) measurement using the vane method (Brookfield YR-1), followed by a slump test (slump diameter in mm) as well as by measuring the exact solids content (% w/w). Following this, a portion of filtrate water was added, in order to slightly decrease the solids concentration, and the resultant slurry was homogenised. A second yield stress measurement and slump test were then performed with the resulting sample and the exact solids content measured again. This procedure was repeated several times until solids content of around 15% w/w was obtained.

Figures 3 and 4 show the relationship between both yield stress and slump diameter versus solids content experimentally obtained for the China clay used within this work program. Both relationships exhibit a strong exponential and linear correlation ($R^2 > 0.9$), respectively. A similar response is obtained when plotting the yield stress versus slump diameter. In this case, however, an inversed logarithmic relationship predominates (Figure 5).

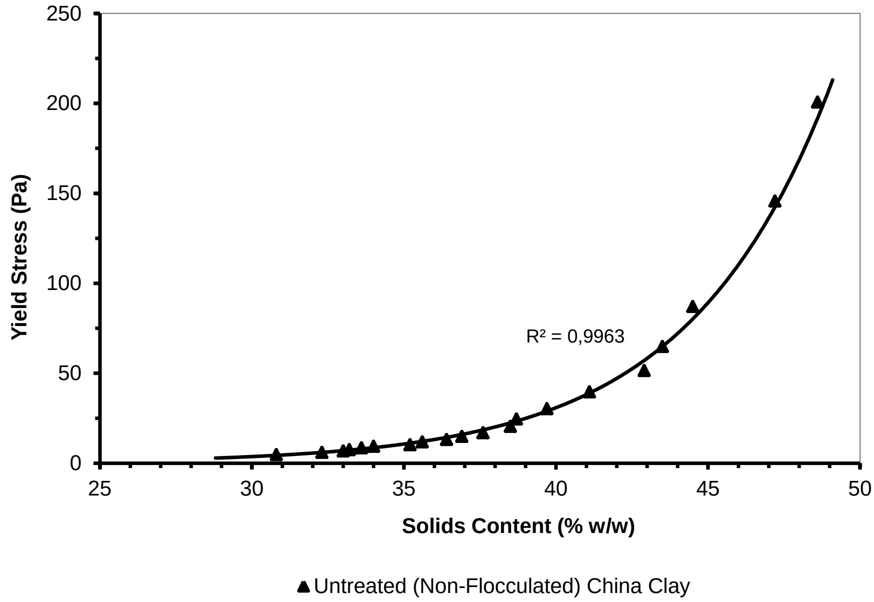

Figure 3 Profile yield stress versus solids content for untreated China clay

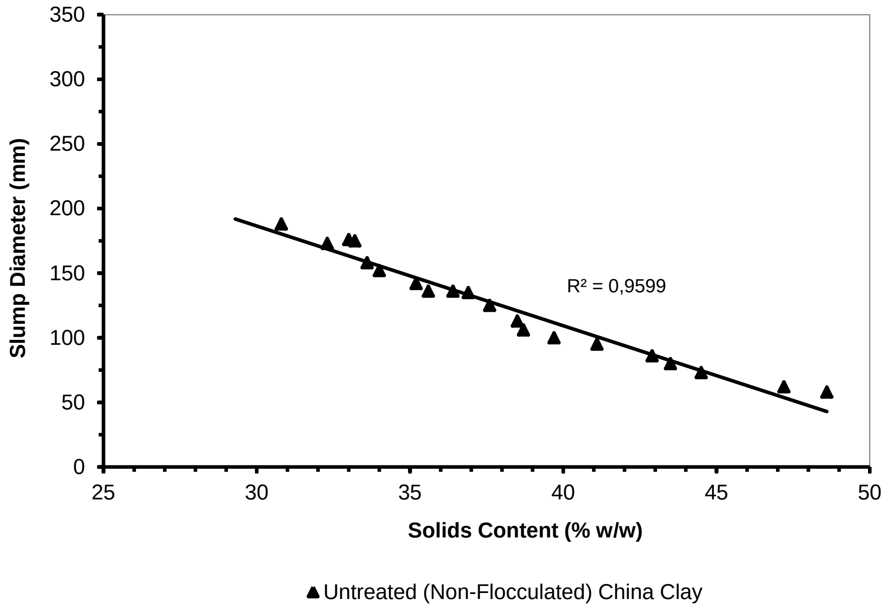

Figure 4 Profile slump diameter versus solids content for untreated China clay

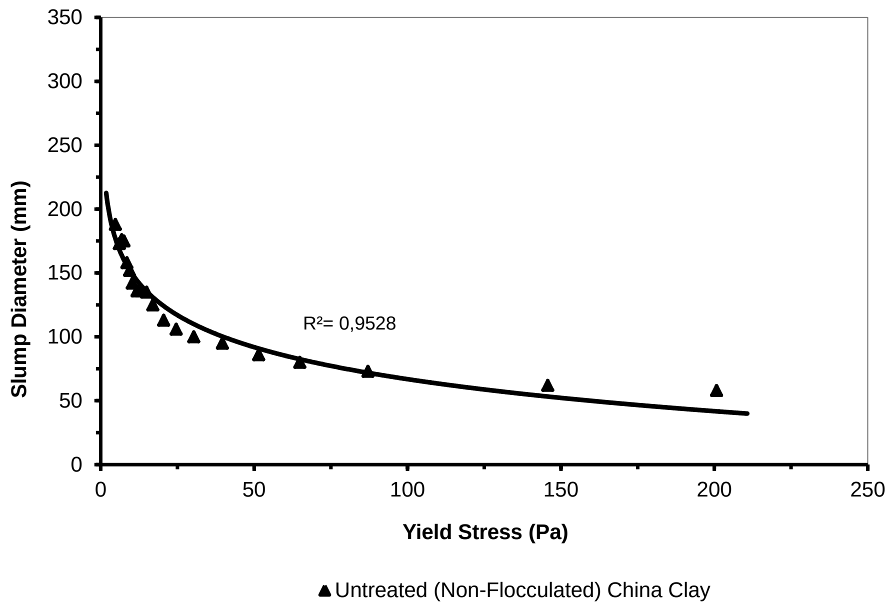

Figure 5 Profile yield stress versus slump diameter for untreated China clay

Note that at approximately 35% w/w solids the yield stress of the China clay was below 10 Pa (Figure 3) and the correlation becomes almost linear. In this regime, the detection/measurement of the yield stress with standard rheometers comprises consistent error and, therefore, the slump test (slump characteristic) becomes a suitable tool (parameter) to use for the indication of the slurry rheology.

Alternatively, at 45% w/w solids and higher, the slump diameter approaches the minimum spread possible to be measured with the mould employed (50 mm) (Figure 2) and the correlation approximates to a horizontal line (Figure 4). In a similar manner, the yield stress and solids content tends to a vertical linear correlation at high solids (Figure 3).

In summary, considering that the consistent correlation between the yield stress and the slump diameter experimentally obtained for the China clay used (R^2 = 0.953) (Figure 5), and that the thickened slurry obtained in our trials did not exceed 30% w/w and that the slump diameter (spread) obtained was considerably larger than the final sample height (H<<<R, as discussed in Section 2.5.3.1), the application of

a slump test with a circular cylindrical vessel and the use of the slump diameter as the indicator of the yield stress of the slurry was justified.

2.7 Flocculants

2.7.1 Conventional flocculant

The conventional flocculant selected was the optimal in terms of dose efficiency and rate of underflow consolidation for the given slurry and process conditions; a commercially available anionic, high molecular weight, acrylic acid/acrylamide-based co-polymer. It was hydrated and diluted in distilled water to a final concentration of approximately 0.015% w/w prior to its application.

2.7.2 BASF NFT

The BASF NFT was prepared under the same conditions and applied in a similar manner to the conventional flocculant system.

2.7.3 Dose

In both systems the dose of flocculant applied was comparable and varied between 120 and 180 g per tonne of dry solids.

3 Results

The relationship between slump diameter (an indirect measurement of yield stress as referenced in Section 2.5.3) and solids content for the untreated feed material, exhibits an excellent linear correlation as shown in Figure 4, even when extended to lower solid contents as demonstrated in Figure 6. In this test work, within the range of solids content investigated, the slump diameter has an inversely proportional linear relationship to the solids content of the slurry and has a line fit with R^2 = 0.965 (Figure 6).

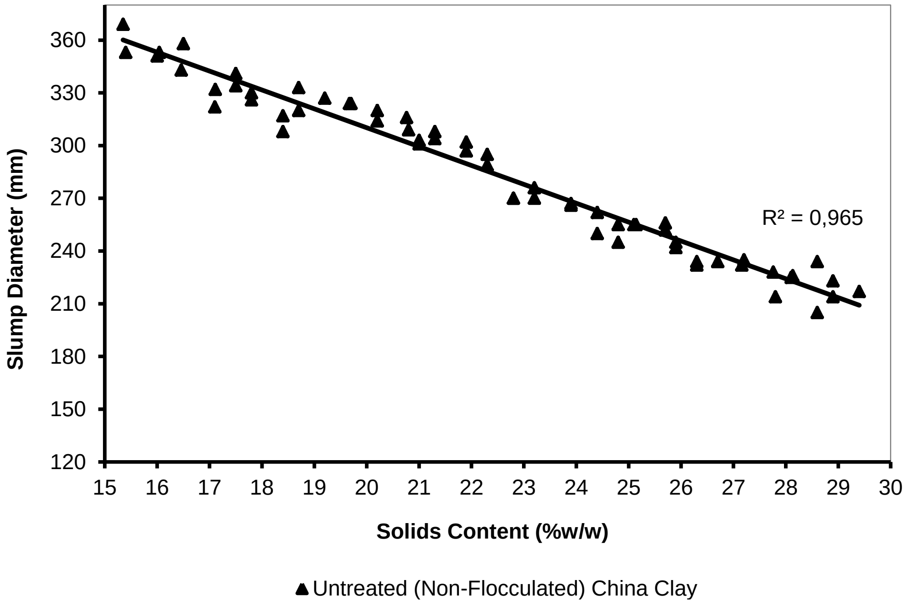

Figure 6 Correlation of underflow slump diameter and solids content

This data represents the 'theoretical minimum' yield stress for a given solids content achievable with the given specific physical/chemical characteristics of the slurry (e.g. particle size distribution, temperature, pH, ionic content). The relationship between slump diameter and solids content for the untreated slurry was subsequently applied as a reference (target) by which to assess the relative performance of both conventional flocculant and BASF NFT on consolidated underflow rheology.

As outlined in Section 2.5.1, an Anton Par DMA 35n densimeter was used to measure the density of the underflow samples produced from each test program. The relationship between slurry density and slurry solids exhibited a strong linear correlation ($R^2 \geq 0.976$), see Figure 7 for details, allowing slurry density measurements to be used in combination with slurry rheological measurement, as an effective means of estimating the relationship and correlation of measured slurry dry solids content and its associated rheological properties.

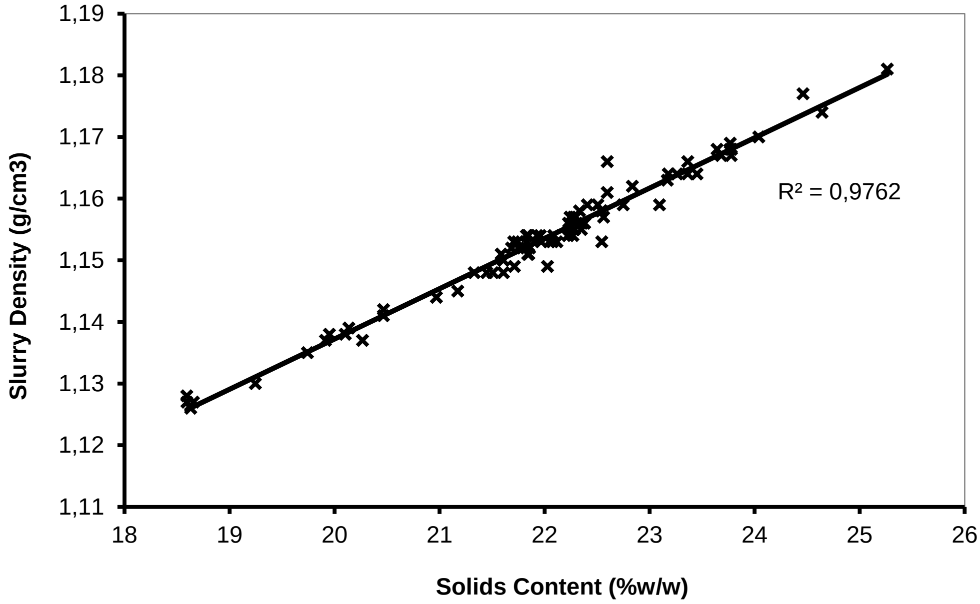

Figure 7 Correlation of underflow slurry density and solids content

The characteristics of the underflow samples taken from the pilot thickener batch tests were initially displayed in terms of underflow solids and underflow rheology (slump diameter) with respect to the chronological order of sample collection. For both conventional flocculant treatment and BASF NFT batch tests, the chronological trends are comparable, in that with time, the underflow solids content and the underflow slurry rheology decrease (slump diameter increases), see Figure 8 for details.

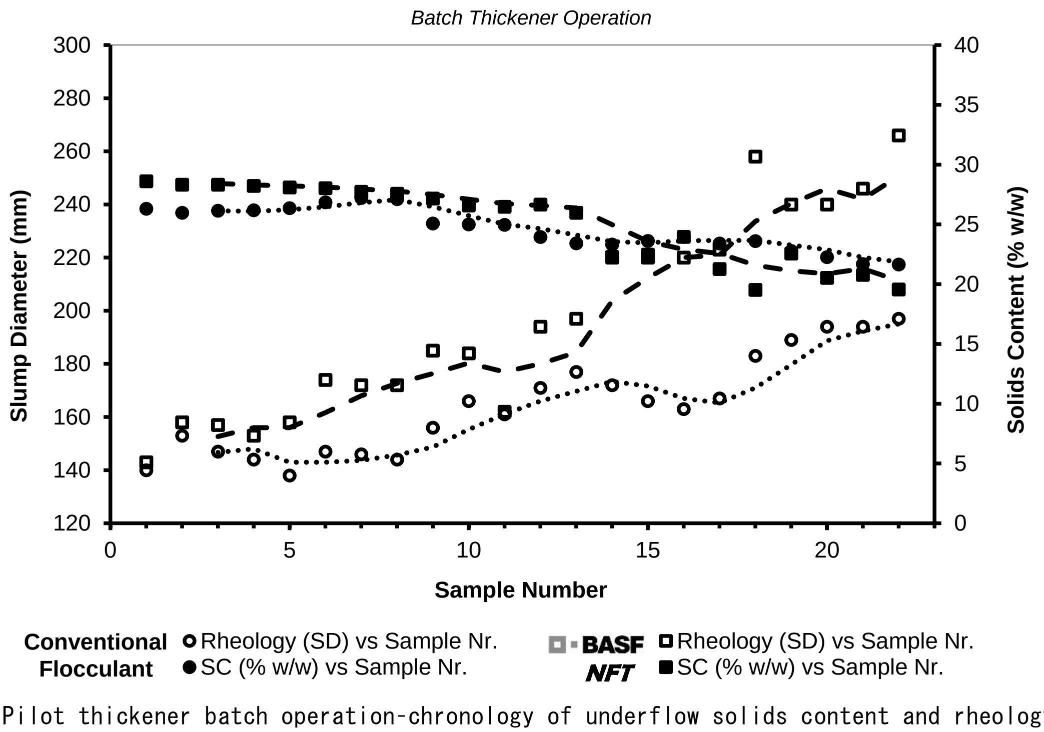

Figure 8 Pilot thickener batch operation-chronology of underflow solids content and rheology

Although both sets of data show some fluctuations from an idealised linear response, the variations are not excessive and their respective trends are as might be predicted.

Performance differences between the conventional flocculant treatment and BASF NFT become apparent when their respective test data is displayed in terms of the relationship between underflow solids and the associated sample rheology. In Figure 9, we see the correlation of this data, both in terms of their respective performance and linear model fits. Untreated China clay and both flocculant treatment systems display inversely proportional linear relationships with fits, $R^2 > 0.9$.

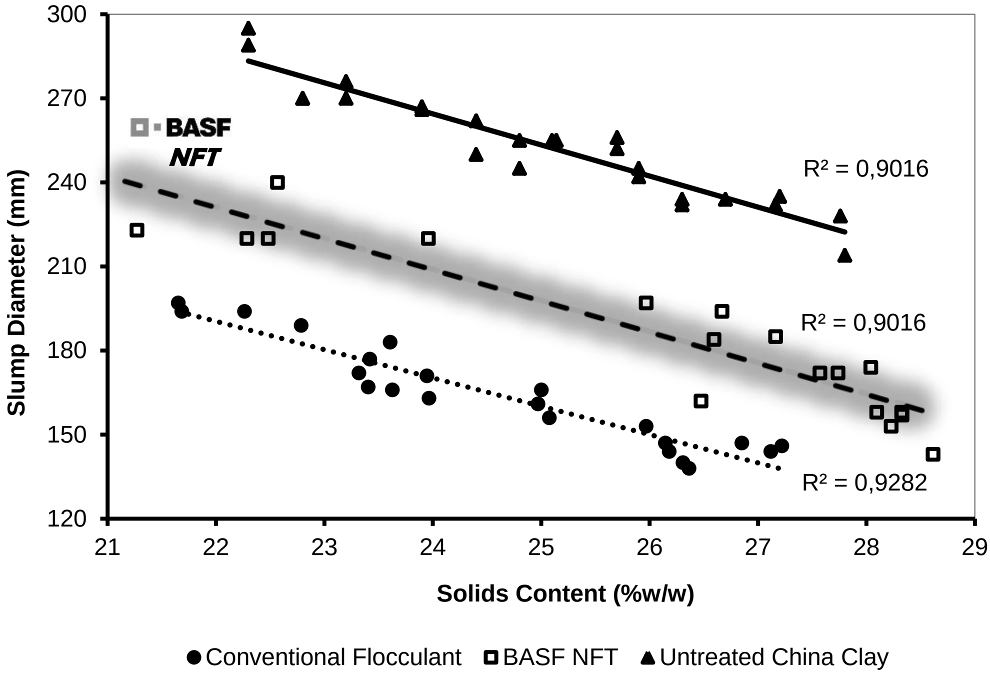

Figure 9 Pilot thickener batch operation-correlation of underflow rheology and solids content

Compared to the conventional flocculant treatment, BASF NFT displays a significant improvement in the underflow solids achievable for a given slurry rheology. Slurry with a slump diameter of 180 mm would be produced by a conventional flocculant treatment containing 23.1% w/w solids, whilst BASF NFT would support a slurry solids content of 26.8% w/w, a 3.7% absolute or a 16% relative increase in associated solids content.

It can be seen that, compared to the conventional flocculant treatment, in terms of slurry rheology for a given solids content, BASF NFT offers a performance that equates to approximately 50% movement towards the 'theoretical minimum' yield stress achievable with the untreated slurry.

Within the pilot thickener dynamic operation, the flocculant system was periodically switched between conventional flocculant and BASF NFT, as indicated in Figure 10. Over a period of approximately 2.5 hours the flocculant was changed six times, alternating between the two treatment systems.

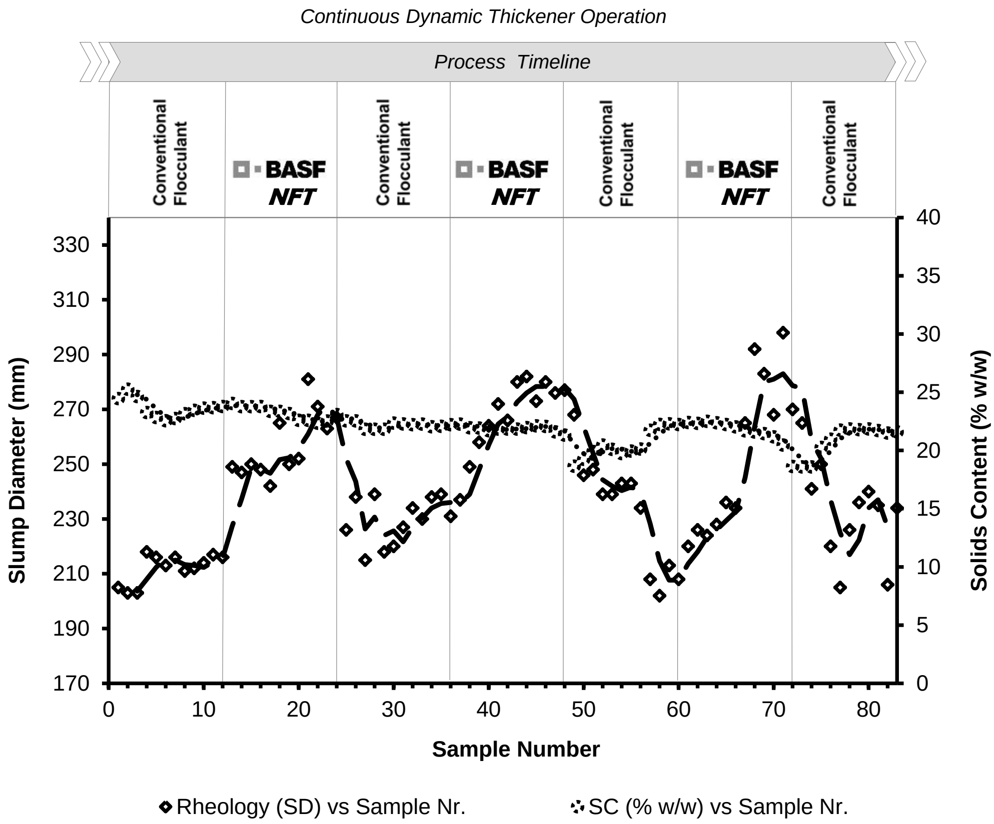

Figure 10 Pilot thickener dynamic operation-chronology of underflow solids content and rheology

As previously conducted within the pilot thickener batch operation, the characteristics of the underflow sample data were initially displayed in terms of underflow solids and underflow rheology (slump diameter) with respect to the chronological order of sample collection.

A significant difference can be seen between the data presented in Figures 8 and 10. The combined data for the conventional flocculant and BASF NFT treatments within the dynamic pilot thickener operation appears to shows a comparable relationship with respect to underflow solids content, in that there is a general reduction in solids content with each sample of underflow taken from the thickener. However, there is a significant fluctuation in the slump diameter when expressed in relation to sample chronology.

When the flocculant treatment changes are overlaid on the timeline, we see a clear correlation between the introduction of BASF NFT and a significant increase in slump diameter (reduction in slurry yield stress).

On each occasion, when the conventional flocculant is introduced into the dynamic pilot thickener operation, there is an associated and significant reduction in underflow slump diameter (increase in slurry yield stress).

There is a clear inference that the application of BASF NFT supports a significant reduction in underflow yield stress. However, further data investigation is required to confirm whether the data responses displayed in Figure 10 are meaningful.

From the data shown in Figures 6 and 9 we demonstrated a correlation between slump diameter and slurry solids content. In the four sets of data shown in these figures there is a strong inversely proportion linear relationship between slump diameter and slurry solids content, in which the line of best fit is consistently $R^2 > 0.9$.

When the data from the dynamic pilot thickener test is displayed in the same way, we see significant scatter in the results and little correlation, see Figure 11. In addition when a linear relationship is applied to the data, the line of best fit is significantly inferior to those derived from the batch tests ($R^2 = 0.127$ compared to those displayed in Figure 9, $R^2 > 0.9$).

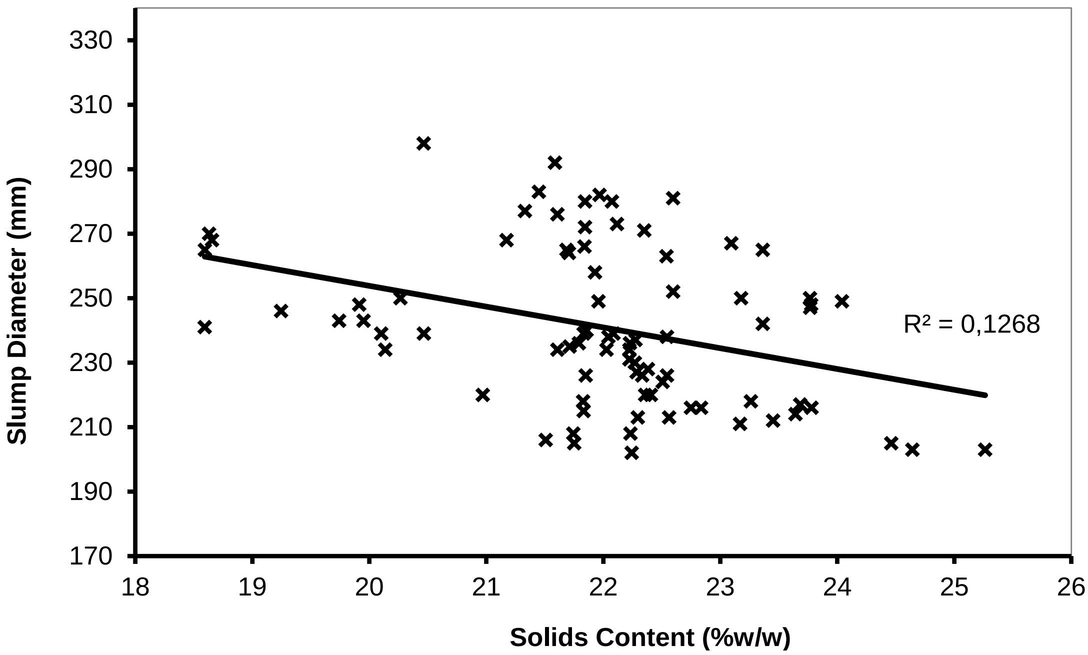

Figure 11 Pilot thickener dynamic operation-correlation of underflow rheology and solids content

This could imply that there is more than one discrete dataset within the viewed results. To investigate this further the test data was divided into two subsets, based upon the chronological times at which the two flocculant systems were applied to the thickener. The results from which, together with comparative data for untreated slurry, can be seen in Figure 12.

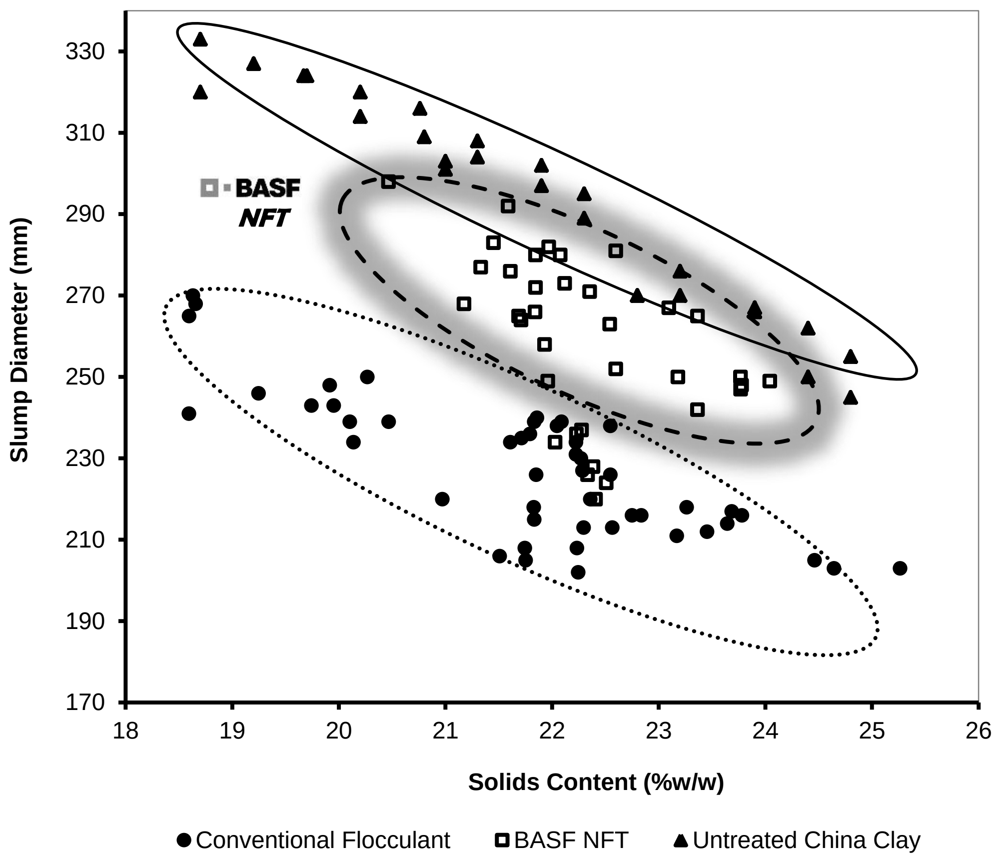

Figure 12 Pilot thickener dynamic operation-slurry rheology for given flocculant treatments

When the dynamic pilot thickener test data is aligned with a specific flocculant treatment system, as shown in Figure 12, we see three discrete underflow slurry rheological profiles. This data, from the dynamic thickener evaluation, corroborates the findings from the earlier batch thickener evaluations, see Figure 9 showing BASF NFT to produce an underflow slurry at a given solids content, that has a significantly higher slump diameter (reduced yield stress) than the equivalent underflow produced with a conventional flocculant.

Perhaps, somewhat surprisingly, when compared to the batch test data, the rheological properties for the BASF NFT treated underflow, generated under dynamic operational conditions, exhibit significant overlap with the properties of the untreated slurry.

4 Conclusions

Both batch and dynamic pilot scale thickening operations have effectively demonstrated the following:

- The application of flocculants, to affect commercially viable gravity settling in continuous thickening operations, modifies the rheological properties of the associated thickener underflow. The flocculated/treated underflow displays a significantly higher yield stress for a given slurry solids content. In thickener systems where rake torque and/or underflow pumping restrictions exist, such changes to consolidated slurry rheology will adversely affect thickener operation.
- The significant difference in rheological properties between conventional flocculant treated and untreated slurries, demonstrates an opportunity to potentially improve the rheological properties of thickener underflows, if the post flocculation effects of high molecular weight polymers can be overcome.
- BASF NFT, when compared to conventional flocculant treatment, offers effective flocculant performance in terms of dose efficiency and rates of underflow consolidation.
- BASF NFT can significantly reduce, and potentially negate, the adverse effect on thickener underflow rheology that is presently generated by conventional flocculants, allowing higher underflow solids to be achieved within the existing operational constraints.

Acknowledgements

The authors and BASF thank AKW Equipment and Process Design for access to their pilot thickener system, laboratory facilities, technical support and general assistance provided during the time of our onsite trials. Thanks also to Amberger Kaolinwerke for providing the China clay substrate from their Hirschau processing facility.

References

Berger, A., Adkins, S., Hess, S., Flanagan, I. and Stocks, P. (2011) Step Change in Underflow Rheology, in Proceedings 14th International Seminar on Paste and Thickened Tailings (Paste2011), R.J. Jewell and A.B. Fourie (eds), 5–7 April 2011, Perth, Australia, Australian Centre for Geomechanics, Perth, pp. 135–142.

Boger, D.V. (2009) Rheology and the Resource Industries, Chemical Engineering Science, Vol. 64, pp. 4525–4536.

Clayton, S., Grice, T.G. and Boger, D.V. (2003) Analysis of the slump test for on-site yield stress measurement of mineral suspensions, International Journal of Mineral Processing, June 2003, Vol. 70, Vol. 1–4, pp. 3–21.

De Kretser, R.G., Boger, D.V. and Scales, P.J. (2003) Compressive Rheology: An Overview, Rheology Reviews, Vol. 165, pp. 125–165.

Pashias, N., Boger, D.V., Summers, J. and Glenister, D.J. (1996) A Fifty Cent Rheometer for Yield Stress Measurement, The Society of Rheology, Inc., Journal of Rheology, November/December 1996, Vol. 40, Vol. 6, pp. 1179–1189.

Roussel, N. and Coussot, P. (2005) Fifty-Cent Rheometer for Yield Stress Measurements: From Slump to Spreading Flow, The Society of Rheology, Inc., Journal of Rheology, May/June 2005, Vol. 49, Vol. 3, pp. 705–718.